International Journal of Chemical and Biochemical Sciences
(ISSN 2226-9614)

Journal Home page:www.iscientific.org/Journal.html

Investigation of Steel's Ability to Resist Corrosion in Multiple Situations

Dhwani Bartwal[1], Aishwary Awasthi[2], Vikas Kumar[3]*

[1]*Department of Agronomy, Parul University, PO Limda, Vadodara, Gujarat, India.*

[2]*Department of Mechanical Engineering, Sanskriti University, Mathura, Uttar Pradesh, India.*

[3]*Department of basic sciences, IIMT University Meerut, Uttar Pradesh, India.*

Abstract

The steel's resistance to corrosion in various settings do study now this paper (industrial water, distilled water, and tap water). Monitoring of each voltage in an open circuit and polarisation curves were used in the study along with irresponsive electrochemical techniques (electrochemical impedance charts). The outcome from Potentiometry with distilled water in the room reveals a modest fluctuation in every corrosion potential, a reduction in cathodic branches, as well as a reduction in the anodic limbs, which result in a substantial decrease in current density and the dissolving away from the steel. High-frequency single capacitive loops, which correlate to a charge transfer process, are what give Nyquist diagrams their distinctive appearance. In the case of distilled water, the resistance to charge transfer Rt rises to 145 Ω.cm2 subsequently declines to 133 Ω.cm2 concerning city water just one continuous time across all media which supports each earlier finding. At high frequencies, the Bode graphs exhibit a resistive region, Optical microscopy is used to analyze the morphologies of the substrate surface.

Keywords: steel, Corrosion, EIS, industrial water, distilled water.

Full length article **Corresponding Author*, e-mail: dhwani.bartwal24197@paruluniversity.ac.in

1. Introduction

Their ability to withstand ordinary corrosion, high-temperature oxidation, and wear and tear while maintaining a high level of strength and ductility, corrosion-resistant steels have a wide range of industrial applications. Austenitic steel that resists corrosion, grade 316L is one of the most widely used steels and is used to make a variety of goods where the highest level of corrosion protection is required. Austenitic stainless steels are often used as structural materials in a variety of sectors, such as steam power, food, biomedical, pipeline, chemical, and heat exchanger equipment industries, because of their superior electrical, thermal, and corrosion resistance [1]. The passive chromium oxide coating that forms on the surface is what gives the material its corrosion resistance. When exposed to hostile conditions, particularly those that include chloride, sulfate, or nitrate ions, this metal can suffer severe corrosion. The fact that it results in significant economic losses around the globe makes this a serious issue that has to be addressed by the business and educational sectors [2]. The amount of carbon in ferritic stainless steel directly affects its ability to resist corrosion. A zone deficient in chromium may form as a result of the proximity of grain boundaries to which chromium carbides precipitate. Hence, at the chromium-depleted zone towards the grain boundaries, Intergranular Corrosion (IGC) occurs [3]. The ability to fully comprehend the rust layers that have grown on the surface of weathering steel is hampered by a lack of data. The main idea behind weathering steel is to employ a protective rust coating to stop the steel from corroding further. In addition to the chemical makeup of the steel, environmental elements of the service condition also affect the protective rust layer's ability to resist corrosion [4]. Corrosion resistance to several possible security hazards and environmental problems concurrently costs substantial economic losses each year. Heavy metals like chromium and nickel, which have detrimental health effects in very tiny doses, are found in significant concentrations in corrosion products. According to NACE 2016, there has been around 2.5 trillion US dollars' worth of economic losses as a result of corrosion. The steel's resistance to corrosion in various environments, the Electrochemical Impedance Spectroscopy (EIS), and every table technique of potentiodynamic polarisation were used (distilled water, city water, industrial water) [5]. Every process of passivation and de-passivation characteristics using a Simulated Concrete Pore Solution (SCPS) Cr-Mo Corrosion Resistance (CR) steel. To characterize the film that is passive's morphology and content, electrochemical techniques, XPS, and AFM

experiments were performed [6]. The influence durability of corrosion resistance of every steel reinforcement into mortars of Red Mud (RM) subjected facing the combined effects of natural carbonation and chloride attack was assessed [7]. Then using various electrochemical experiments along with surface characterization approaches, the impact of Phytate Ions (IP6) on carbon steel corrosion resistance in imitation concrete pore solutions including and without passive coatings was examined [8]. The primary contributing component to the protectiveness of a scale generated by [9] high temperature and pH under CO2-saturated circumstances is identified using electrochemical and surface analysis methods. The paper [10] increased the corrosion resistance and surface hardness of a Carbon Steel (CS) substrate with an electrodeposited multilayer composite covering made of Nickel-Phosphorus (Ni-P) and Nano-ZnO. Through using electrochemical processes, surface analysis, and the impact of the chloride ion on the metal's capacity to withstand corrosion Ni-advanced rusting steel in a synthetic tropical environment move examined [11]. The cyclic corrosion test, dry/wet was [12] used to look at the impact of Corrosion resistance (Cr) on weathering steel's ability to resist a tropical marine environment simulation's corrosion. The paper [13] suggested that cement-based materials can be made more corrosion-resistant by adding super-hydrophobic modified steel slag to reduce water absorption. Through means of simple mechanical agitation, a composite material made Comprising Modified Nano Titanium Dioxide (TiO2-KH550), Reduced Graphene Oxide (rGO), and Polyvinyl Butyral (PVB) do create by [14]. The article [15] presented a unique ternary Cement Polymer Composite Coating (CPFNIC) for steel rebars in chloride environments that contain nanoparticles, an inhibitor, and fly ash. The phosphorus-free corrosion inhibitors for carbon steel in soft water, dendritic polymers with an Isothiourea Terminal group, a Carboxyl lateral group, and Pentitol core dendrimers of generations 0 and 1 (ITCP-0G and ITCP-1G) were created [16]. The article [17] focused on the spontaneous production of passive coatings on Low Carbon (LC) steel and 10% Cr steel at different molybdate concentrations with significant chloride contamination in an alkaline solid stone pore solution. With LC steel, molybdate prevents corrosion brought on by chloride, and this effect becomes more prominent with higher molybdate concentrations and longer immersion times.

2. Materials and methods

2.1 Components

Table 1 provides a breakdown of the steel substrate's chemical makeup used in this investigation. They are interested in the steel's corrosion during three diverse environments: purified water, municipal water (ANNABA) as well as industrial water from all national businesses METAL ARCELOR ARCELOR (ANNABA). Every sample used in the electrochemical testing had a bottom surface area of 0.5 cm2 and was implanted in epoxy resin. The working electrode is subjected to a pretreatment procedure before each test that entails mechanically polishing abrasive sheets on the surface of varying grades (90 to 3000), washing and degreasing with acetone, followed by rinsing with distilled water and airflow to dry [18].

2.2 Electrochemical measurements

A potentiostat/galvanostat Autolab 302N model, together with the software a standard three-electrode electrochemical cell, and Nova 2, were used to conduct the electrochemical measurements: the platinum counter electrode, every reference electrode known as each Saturated Calomel Electrode (SCE), every low carbon functioning electrode made of steel. The experiment was carried out in a static environment with the test solutions exposed to air. Throughout the experiment, 298 K was maintained as the temperature of the solutions. After one hour of immersion in the solution, potentiodynamic curves are displayed at a scan speed in the potential range of 1 mV/s (-250 to +250) mV/ECS. Every acquired polarisation curve at ±10 mV with corrosion potential was used to calculate the polarisation Resistance (Rp). The amplitude, and Electrochemical Impedance Spectroscopy (EIS) measurements were performed at the open circuit potential in the 100 kHz to 10 MHz frequency range [19].

2.3 Surface analysis

An optical microscope, the NICON Eclipse LV150N, was accustomed to examining the shape of steel's surface after it had been immersed for 48 hours in three distinct conditions [20].

3. Results and Discussions

3.1 The untapped potential is observed

The crucial to track how the untapped potential changes over time in various settings, up until it reaches stability. Every reaction that takes occur on the metal's surface determines this potential's values. Figure 1 illustrates this progression. The sample corrosion with the creation of corrosion products is characterized by the changing probability of testing into various settings (D.W, I.W, and C.W). While submerged for two hours and at a value of -140mV/ECS, they notice an enhancement of the potential (Ecorr) in the existence of distilled water with good stability.

3.2 Polarization curves

Figure 2 displays each steel's polarisation curves after 2 hours of immersion in various settings at a scan rate of 1 mV/s. The polarization curves for steel in various conditions are shown in Figure 2. They see that the current densities drop, notably for distilled water, when Corrosion potential rises in direction of positive values. The dissolving of iron occurs during the anodic and cathodic processes of steel corrosion.

$$Fe \rightarrow Fe^{2+} + 2e^{-} \quad (1)$$

Table 1. Chemical composition of the steel

Eléments	C	Si	Mn	P	S	Al	Cr	Ni	V
Composition (wt. %)	0.4	1.58	0.76	0.019	0.012	0.210	26.96	11.25	0.010

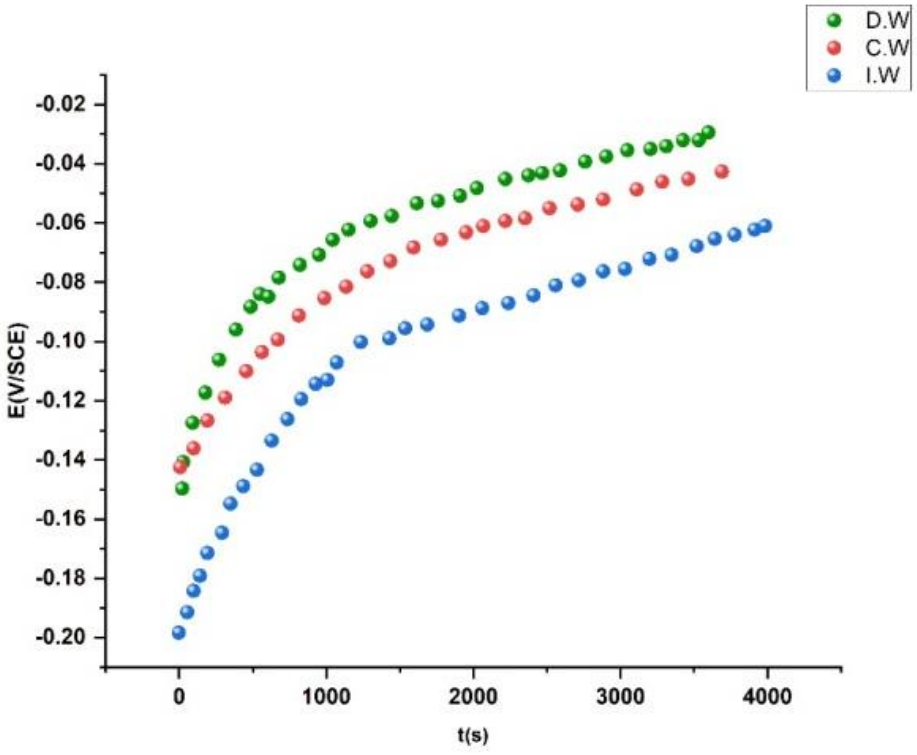

Figure 1. Monitoring of the open circuit potential of steel immersed in different Environments (D.W, I.W, and C.W).

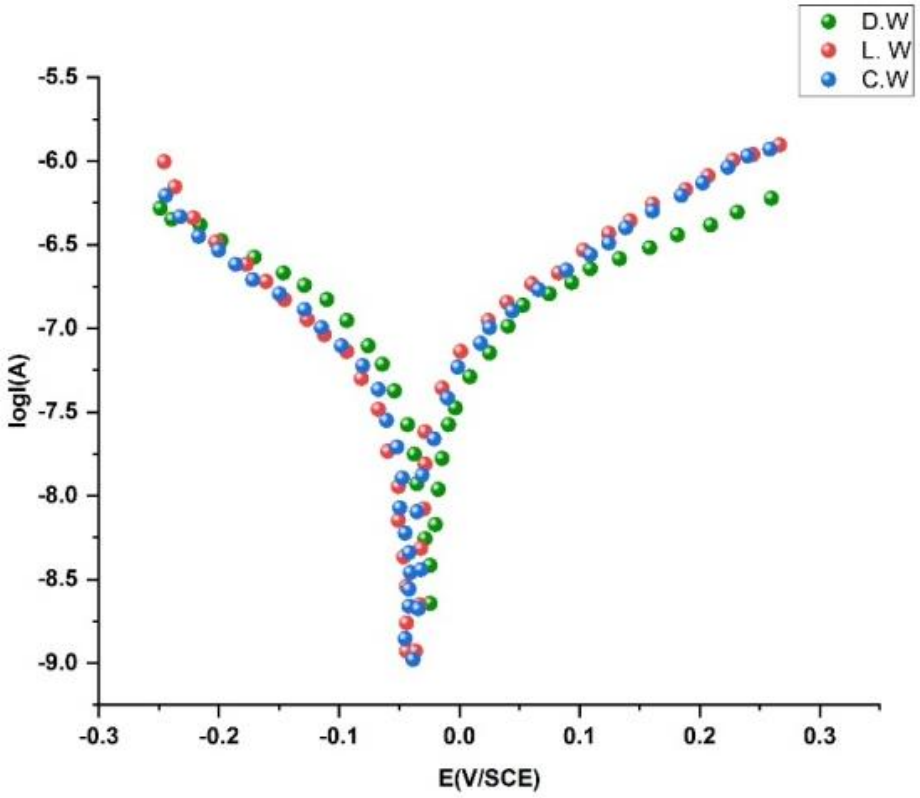

Figure 2. Steel polarization curves exposed to various conditions

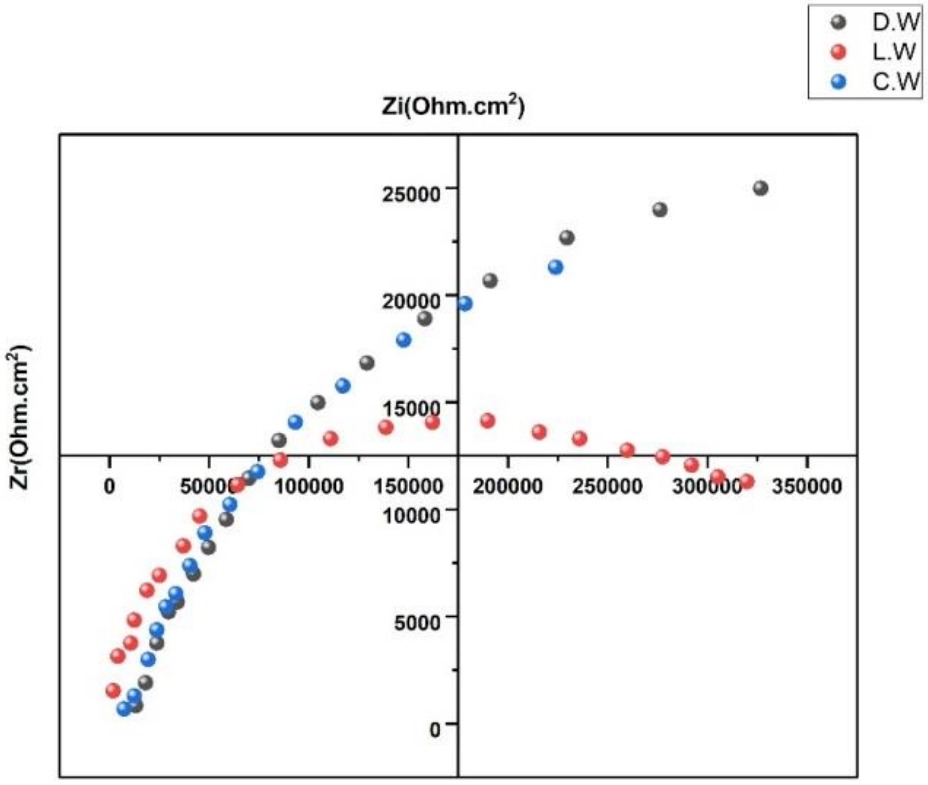

Figure 3 (a). Electrochemical of Nyquist

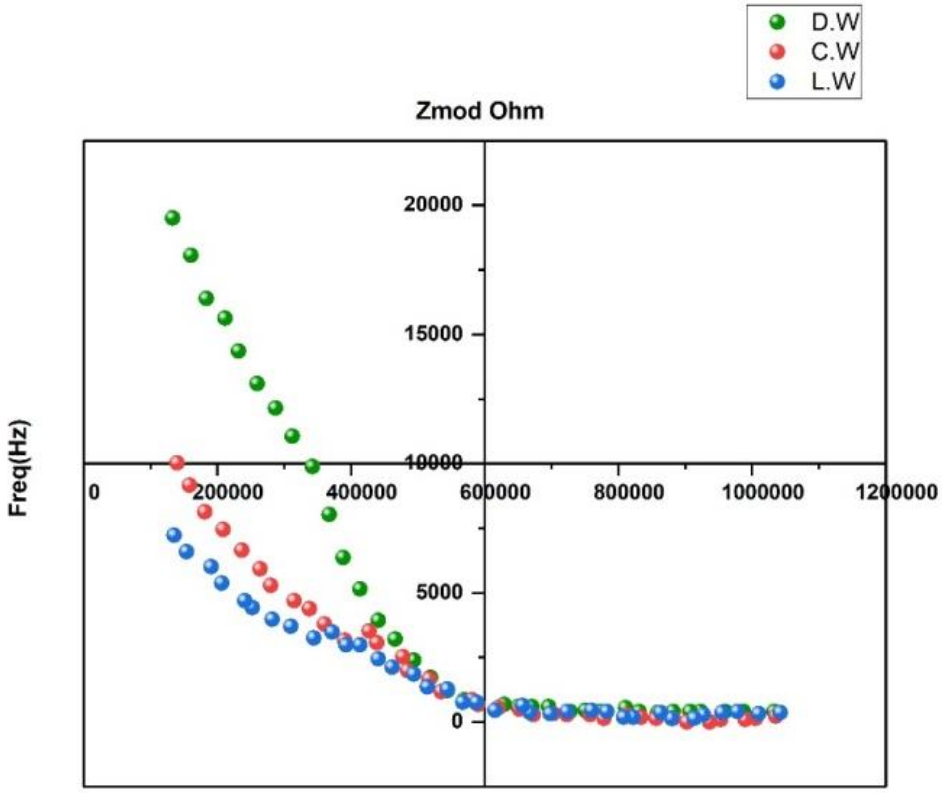

Figure 3 (b). A resistive region

Table 2. Different solutions' conductivity and pH values

Solutions	pH	C(s/m)
D.W	7.84	0.52
I.W	6.51	2.02
C.W	5.44	1.05

Table 3. Electrochemical parameters deduced from the polarization curves of steel in different environments (D.W, I.W, C.W)

Solutions	$B_a(V/dec)$	$B_c(V/dec)$	$E_{corr,cal}$ (v)	$E_{corr,obs}$ (v)	I_{corr} (A)	W(mm/y)	R_p ($\Omega.cm^2$)	E_i (V/SCE)	E_i(V/SCE)
D.W	0.127	0.117	-0.033	-0.033	$2.047.10^{-8}$	0.00025	$9.969.10^{5}$	-0.094	0.041
I.W	0.122	0.119	-0.042	-0.042	$2.592.10^{-8}$	0.00032	$8.344.10^{5}$	-0.088	0.023
C.W	0.087	0.082	-0.049	-0.045	$3.186.10^{-8}$	0.00035	$8.973.10^{5}$	-0.081	0.000

With the decrease of oxygen:

$$O_2 + 2H_2O + 2e^- \rightarrow H_2O_2 + 2OH^- \quad (2)$$

$$H_2O_2 + 2e^- \rightarrow 2OH^- \quad (3)$$

Hence, when iron hydroxide forms close to a metal surface:

$$Fe^{2+} + 2OH^- \rightarrow Fe(OH)_2 \quad (4)$$

In the presence of distilled water, we see and remark the following according to the electrochemical parameter values:

-An increase now positive values of each corrosion potential *(Ecorr)*

$$0.047m\frac{V}{ECS}to - 0.031m\,V/ECS$$

A reduction in current density *(color)* to 2.049.10-8A as the absolute minimum

The polarization resistance (Rp) is raised to the highest possible level of $9.967.10^5\pi.cm^2$

3.3 Electrochemical impedance spectroscopy

With the Autolab 302N corrosion analyzer chain and NOVA 2 software, we generated electrochemical impedance diagrams at corrosion potential to better understand the mechanisms causing corrosion on the steel surface in various settings. These spectra, which have amplitudes of 10 mV and a range of frequencies between 100 kHz and 10 MHz, were collected after two hours of immersion, at the open circuit potential. They are shown in Nyquist diagrams (Figure.3.a.), where a single semicircular capacitive loop is present and grows in size, particularly in distilled water, as a result of the electrode's progressive creation of a protective coating; this charge transfer controls a rusting process phenomena [17].
Inside each diagram of Bode, they observe:
Figure 3b shows an area of resistance with a rising charge transfer resistance at high frequencies. Figure 3c shows just a one-time constant is displayed in each scenario.

3.4 Surface condition characterization

3.4.1 Optical microscopy analysis

A NICON Eclipse LV150N optical microscope was used to examine the steel's surface morphology that was submerged because two hours equal three distinct conditions. The application of an optical microscope observation reveals such: Within twain settings (C.W, I.W). In Figures 4b and c, the emergence is visible in thick regions such are the result of the development of corrosion products. When distilled water is present, however Figure 4a, each whole surface is homogeneous and roughness is minimal. The production of an oxide layer that protects the steel's surface may be linked to this development. Several researchers have reported experiencing similar findings.

4. Conclusions

The test's potential evolution in distilled water revealed the production of corrosion products. Distilled water exhibits a more pronounced ennobling of potential, which leads to the creation protective nature coating. A reduction in each cathodic and also anodic branch. The electrochemical impedance diagrams demonstrated that there was just one capacitive loop. According to the MO findings, the oxide film's production has significantly reduced the steel surface's roughness.

References

[1] S.M. Mohamed, M.M. Sanad, T. Mattar, M.F. El-Shahat, C. Rossignol, L. Dessemond, K. Zaidat and S. Obbade, (2022). The structural, thermal, and electrochemical properties of MnFe1− x-yCuxNiyCoO4 spinel protective layers in interconnects of solid oxide fuel cells (SOFCs).Journal of Alloys and Compounds, 923:166351.

[2] L. Pan, C.T. Kwok, B. Niu, X. Huang, Y. Cao, X. Zou, and J. Yi, (2023). Enhancement in hardness and corrosion resistance of directed energy deposited 17–4 PH martensitic stainless steel via heat treatment. Journal of Materials Research and Technology, 23: 1296-1311.

[3] J. Fu, J. Wang, F. Li, K. Cui, X. Du, and Y. Wu, (2020). Effect of Nb addition on the microstructure and corrosion resistance of ferritic stainless steel. Applied Physics A, 126:1-12.

[4] X. Yang, Y. Yang, M. Sun, J. Jia, X. Cheng, Z. Pei, Q. Li, D. Xu, K. Xiao and X. Li, (2022). A new understanding of the effect of Cr on the corrosion resistance evolution of weathering steel based on big data technology. Journal of Materials Science & Technology, 104: 67-80.

[5] N. Yang, T. Yang, W. Wang, H. Chen and W. Li, (2019). Polydopamine-modified polyaniline-graphene oxide composite for enhancement of corrosion resistance. Journal of hazardous materials, 377:142-151

[6] Z. Jin, C. Xiong, T. Zhao, Y. Du, X. Zhang, N. Li, Y. Yu, and P. Wang, (2022). Passivation and de passivation properties of Cr–Mo alloyed corrosion-resistant steel in simulated concrete pore solution. Cement and Concrete Composites, 126:104375.

[7] J. Shi, X. Guan, J. Ming and X. Zhou, (2022). The improved corrosion resistance of reinforcing steel in mortars containing red mud after long-term exposure to aggressive environments. Cement and Concrete Composites, 130:104522.

[8] Y. Liu and J. Shi, (2022). The corrosion resistance of carbon steel in alkaline concrete pore solutions containing phytate and chloride ions. Corrosion Science, 205:110451.

[9] R. De Motte, E. Basilico, R. Mingant, J. Kittel, F. Ropital, P. Combrade, S. Necib, V. Deydier, D. Crusset and S. Marcelin, (2020). A study by electrochemical impedance spectroscopy and surface analysis of corrosion product layers formed during CO2 corrosion of low alloy steel. Corrosion Science, 172:108666.

[10] N. Jiang, Y. Liu, X.N. Yu, H.B. Zhang, and M.M. Wang, (2020). The corrosion resistance of nickel-phosphorus/nano-ZnO composite multilayer coating electrodeposited on carbon steel in acidic chloride environments. Int. J. Electrochem. Sci, 15:5520-5528.

[11] Y. Fan, W. Liu, Z. Sun, T. Chowwanonthapunya, Y. Zhao, B. Dong, T. Zhang, and W. Banthukul, (2021). Effect of chloride ion on corrosion resistance of Ni-advanced weathering steel in simulated tropical marine atmosphere. Construction and Building Materials, 266:120937.

[12] M. Sun, C. Du, Z. Liu, C. Liu, X. Li and Y. Wu, (2021). Fundamental understanding of the effect of Cr on corrosion resistance of weathering steel in simulated tropical marine atmosphere. Corrosion Science, 186:109427.

[13] Z. Shi, Q. Wang, X. Li, L. Lei, L. Qu, J. Mao and H. Zhang, (2022). Utilization of super-hydrophobic steel slag in mortar to improve water repellency and corrosion resistance. Journal of Cleaner Production, 341:130783.

[14] Z. Zhu, S. Chen, Y. Zhang, and W. Wang, (2022). Corrosion resistance of polyvinyl butyral/reduced graphene oxide/titanium dioxide composite coatings for stainless steel in different environments. Progress in Organic Coatings, 173:107226.

[15] M. Harilal, R.P. George, S.K. Albert, and J. Philip, (2022). A new ternary composite steel rebar coating for enhanced corrosion resistance in chloride environment. Construction and Building Materials, 320:126307.

[16] H. Zheng, B. Zhang, X. Wang, Y. Lu, F. Li and C. Li, (2023). Improved corrosion resistance of carbon steel in soft water with dendritic-polymer corrosion inhibitors. Chemical Engineering Journal, 452:139043.

[17] M. Wu and J. Shi, (2021). Beneficial and detrimental impacts of molybdate on corrosion resistance of steels in alkaline concrete pore solution with high chloride contamination. Corrosion Science, 183:109326.

[18] L. Huang, K.P. Yang, Q. Zhao, H.J. Li, J.Y. Wang and Y.C. Wu, (2022). Corrosion resistance and antibacterial activity of procyanidin B2 as a novel environment-friendly inhibitor for Q235 steel in 1 M HCl solution. Bioelectrochemistry, 143:107969.

[19] Y. Ma, Q. Sun, S. Wang, Y. Zhou, D. Song, H. Zhang, X. Shi and L. Zhang, (2022). Li salt initiated in-situ polymerized solid polymer electrolyte: new insights via in-situ electrochemical impedance spectroscopy. Chemical Engineering Journal, 429:132483.

[20] X. Gu, Y. Zhuang and D. Huang, (2022). Corrosion behaviors related to the microstructural evolutions of as-cast Al0. 3CoCrFeNi high entropy alloy with addition of Si and Ti elements. Intermetallics, 147:107600.